*Statistical Methods in Healthcare. Eds.*Frederick Faltin, Ron Kenett, Fabrizzio Ruggeri, to be published by John Wiley & Sons, Inc

"Interactive Clinical Trial Design": A Combined Mathematical and Statistical Simulation Method for Optimizing Drug Development

Zvia Agur

Optimata Ltd., 7 Aba Hillel St., Ramat Gan, 52522, and Institute for Medical Biomathematics (IMBM), 10 HaTe'ena St., Bene Ataroth, 60991, Israel

Abstract

Clinical trials have been traditionally carried out in a "trial and error" fashion, which is highly inefficient in measures of human and animal suffering, cost and time to market of the newly discovered compounds. Currently, pharmaceutical companies investigate various methods for increasing their productivity in drug development, in order to compensate for increasing costs and to avoid regulatory fiascos.

The major drawback of the traditional system lies in the lack of *a priori* guidance about the potentially successful treatments. The need for a change in paradigm of clinical trial design has been reiterated, and it has been suggested that the new paradigm should be based on formal methods for predicting disease progression under specific treatment regimens of given drugs or drug combinations.

A complex set of mathematical models, denoted *Virtual Patient Model*, retrieving the dynamics of key biological, pathological and pharmacological processes in the body of a patient undergoing anti cancer drug treatment has been developed. The Virtual Patient Model has been employed for studying improved regimens for cytotoxic and cytostatic mono- and combination drug regimens and for selecting optimal personalized treatments. By simulating in the Virtual Patient Model in a population of patients, one can conduct Virtual Clinical Trials recreating and improving drug development. To this end a collection of Virtual Patients Models is created (denoted Synthetic Human Population). Each Virtual Patient in the population is represented

by a set of parameters for the Virtual Patient Model. The inclusive set of parameters represents the distributions of disease, physiological and PK/PD parameters in the population. The Virtual Clinical Trials can be employed in drug development in conjunction with an elaborate algorithm, Interactive Clinical Trial Design (ICTD), which provides a method for a step-by-step process of model prediction and in-vivo verification. The user can employ the ICTD for fine-tuning and testing the drug/disease/population models interactively with the "real" clinical trials, so that relatively early during development the Virtual Patient Model can be employed for checking the most appropriate treatment schedules for the drug, or for making an early "No-Go" decision. The ICTD algorithm is expected to replace the current drug trial-and-error policy by a new policy of clinical trials, which will be based upon a gradual improvement and zeroing-in on the best prediction-directed treatment schedules.

Table of Contents

1. **Introduction**

The number of new drugs brought into the market has dropped significantly in the last few years, despite the substantial effort of pharmaceutical companies in medical research and development and in capital investments. In addition, the regulatory agencies have become more cautious about approving new molecular entities, in the wake of several fiascos of new. The resulting depleted pipelines may have serious consequences for industry, society and government, and a big crisis is foreseen if drug development becomes too risky and unprofitable. If the Pharmaceutical industry is to remain at the forefront of medical research and continue helping patients, it must become more innovative in reducing the development time and costs of new therapies ("Pharma 2020 - Which path will you take?" (PriceWaterhouseCoopers, Report 2008).

Currently, the physical and toxicological properties of drug candidates are mostly studied in vitro, by screens to find molecules that "hit" a designated target. The most promising candidates are then selected to be tested in animals, and subsequently, in large scale clinical trials, essentially conducted by 'trial and error'. Pharmacometric research develops models for the response-time profiles observed in a clinical trial. These models may be then used for designing further clinical studies, for deciding upon dosing strategies and for other developmental decisions. Pharmacometrics also analyzes dose-concentration-response data from trials to understand therapies with existing drugs, with the aim of allowing improved therapy. However, Pharmacometrics analyses are mostly retrospective, relying on large data bases obtained during the clinical trials. The Pharmaceutical industry needs a faster, cheaper and more predictive way of testing molecules before they go into the clinic.
One strategy is to use "virtual R&D," i.e., R&D aided by computer simulations of the human body, to dramatically shorten the period of development of new drugs, and substantially reduce the chance of clinical failure, for substantially reducing costs across clinical development.

Research shows that drug effects may crucially depend on the internal dynamics of the cancer growth processes, as well as on the relevant patient's physiology. These aspects might often be too complex to be estimated by the naked eye, and slight changes in the treatment schedule may be critical for the effect (1-4). In theory, if all potential treatment schedules could be tested, considering all the available information on the involved biological processes, pathological processes and the momentary effect of the drug on every element of these processes, one could, a-priori, suggest a theoretical set of the most promising treatment schedules for a given indication, or, even, for a given patient. Subsequently, these promising schedules would be clinically tested, thus saving human resources and time, and helping to achieve maximal possible therapeutic effects of the tested drug.

Moreover, such a method would enable to take off the shelf drugs with valid properties, which failed during the development process, due to insufficient efficacy, or limitations of toxicity, which could possibly be overcome by modifying the treatment schedule. In addition, it would enable a Go–NoGo decision to be made early during the clinical trial process.

In this chapter we will discuss the development of the Virtual Patient Model, and its use for identifying improved drug schedules. The Virtual Patient Model of a solid cancer disease includes a mathematical model of tumor progression, and we will explain how such a model is constructed and simulated. We will briefly describe retrospective clinical validation of the basic Virtual Patient model. Subsequently, we will discuss how Synthetic Human Populations (SHP) are created that transfer the real-life distribution of parameters into the Virtual Patient model. *Interactive Clinical Trial Design*^{TM} (ICTD; (5), for use of the SHP-implemented Virtual Patient Model in virtual clinical trials, will be discussed and compared to adaptive clinical trials. The ICTD involves massive simulations of a population of the Virtual Patient Models, reflecting the patient population (to be denoted *Synthetic Human Population*). The ICTD enables the drug developer to generate, fine-tune and validate a reliable drug/disease/host model for forecasting improved treatments during an ongoing

"real" clinical trial. Thus, relatively early during development, i.e., by the end of Phase-I, and no later than in mid-Phase-II, the model already contains the PK/PD drug parameters, to be embedded in the Virtual Patient Model. At this stage numerous drug schedules, termed "infinite regimen space", are simulated for any desired indication, and optimization methods are employed for selecting, among the vast number of simulation scenarios, those yielding best results according to the list of specifications set by the drug developer. This method carries little risk of yielding false predictions, since the algorithm has been designed so as to be continuously validated and improved by information derived in parallel from clinical trials.

In this way one can identify the most appropriate patient-population/schedule for the drug, or alternatively, make a "NoGo" decision. The method is expected to replace the current drug trial policy, essentially one of "shots in the dark," by a new policy of rationally designed clinical trials, which will be based upon a gradual improvement and zeroing-in on the best prediction-directed treatment schedules.

2. Development of the Virtual Patient Concept

The Virtual Patient model (Fig 1) is a set of multi-scale mathematical models that describe disease progression and the progression of relevant physiological toxicity processes. These models are simulated in conjunction with pharmacological models, fully accounting for the pharmacokinetics/pharmacodynamics (PK/PD) and dosing regimens of specific drugs or drug combinations. Simulation results are used for predicting the efficacy and toxicity of the drug under multitudes of putative treatment regimens. In addition, the platform of the Virtual Patient model includes powerful optimization algorithms, which select the best treatment for specific patient population, out of a large number of potential treatments.

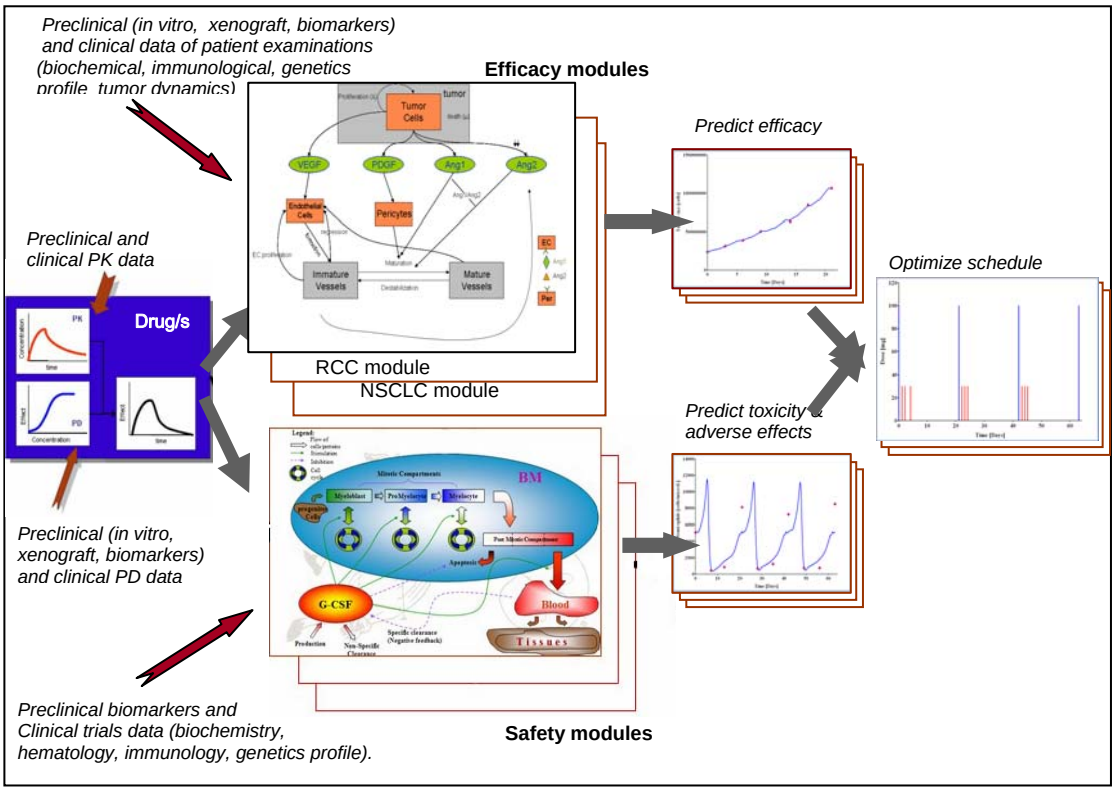

Figure 1. The Virtual Patient of a vascular cancer disease in a nutshell.
Mathematical models for the PK and the PD of the drug(s) are derived based on the available preclinical information (left panel). These are integrated into the mechanistic multiscale disease model and the relevant toxicity models. The latter are multilevel models describing molecular, cellular, tissue dynamics and the interaction between them. The PK\PD models integrated into the relevant biological process models are now simulated over a large range of potential treatment regimens, and regimen-associated efficacy and toxicity are predicted. Finally (right panel) powerful optimization algorithms are used for identifying the most appropriate drug regimen for particular endpoints set by the drug developer.

2.1 The basic Virtual Patient Model

In the 1980s Agur suggested a mathematical model, which takes account of cell-cycle dynamics of tumor and host cellular dynamics. The model suggested that intermittent delivery of cell-cycle phase-specific drugs, at intervals equivalent to the mean cell-cycle time, might minimize harmful toxicity without compromising therapeutic effects on target cells (*Z-Method* (6-7)). Subsequently, explicit general formulae have been derived for the growth or decay of cell populations that are subjected to repeated pulse delivery of cell-cycle phase-specific drugs (2), and an algorithm has been developed for calculating the required length of treatment for this regimen (8).

On the basis of the above theory Agur and colleagues (9) have developed a heuristic optimization method, which uses Operations Research techniques for identifying improved drug schedules in any group of patients. The work focuses on developing the general concept of the optimization method, rather than on the particular implementation and hence, the much simplified, but already validated, cell-cycle model, briefly mentioned above and described below, was selected for describing disease progression. The heuristic optimization method resulting from this simplified approach admits dynamic mathematical models of any desired level of complexity and is employed by the Interactive Clinical Trial Design™ (ICTD) method, also to be described below.

The cell-cycle model, considers two types of target cells in the human body. The host cells, denoted h-cells, and the malignant cells denoted m-cells, which are, in fact, the tumor. Both types of cells may be damaged when exposed to drug treatment. Our aim is to reduce the number of m-cells, while maintaining a certain level of h-cells in the body. We assume that the lengths of the cell-cycle phases are deterministic and known, both for host and malignant cells. Both host and malignant cells are susceptible to the drug during some of the cell-cycle phases, denoted here the critical cell cycle phases. If a cell is exposed to drug treatment, typically chemotherapy, during part of its critical phase there is a chance that it will be eliminated.

Specifically, we assume that during each unit of time in which treatment is applied, a fraction of the cells which are in their critical phase will be eliminated. Our aim is to reduce the number of m-cells to a certain fraction of their initial level. However, in order not to cause irreversible damage to the patient, we must schedule treatments so that the number of h-cells will always remain above a fraction of its initial level. Cells of both types multiply, but not necessarily at the same rate. If the number of m-cells is reduced below the desired level, we assume that the remaining m-cells will not multiply anymore.

We assume that treatments can be of variable length and can be given at any time. A solution, i.e., a treatment schedule, determines those time intervals in which treatment is to be applied. This model is computationally intractable, as it is proved to be NP-complete, even in extremely simplified special cases. Consequently, an approach was put forward, aimed at obtaining good solutions that are not necessarily optimal. The approach solves the model by applying local search heuristics (9).

2.1.1 A simple cancer progression model

Let us denote by τ_i and s_i the length of the cell cycle and the Critical phase, respectively, of i-cells, $i \in \{a, h\}$. At the end of the cell cycle the cell may produce daughter cells. The average number of daughter cells produced by a single i-cell that reaches age τ_i is the growth rate in the i-cells' population and we denote it by r_i.

If the proportion of m-cells is reduced to a fraction β_a of its initial level, then the patient is considered cured and the treatment may be stopped. In practice, the proportion of h-cells must remain above a fraction β_h of its initial level during the entire treatment. If the proportion of h-cells falls below this level, the patient is considered dead. However, we will allow solutions that do not satisfy this condition to be tested, with the aim of achieving good solutions at a later stage of the process. In our model, the patient can only die as a result of the treatments' toxicity - death is not caused by the tumor. This model assumption would not result in solutions that

leave a patient without treatment, since growing cancer cells will quickly reduce the fitness to $-\infty$. Hence, solutions that result in a patients' death due to treatment have higher fitness values than solutions that do not treat the patient at all.

For each $t \in [0,T]$, the state of the system is characterized by two ``density'' functions, $n_i(w,t)$ $i \in \{a,h\}$, that are defined for $w \in [0,\tau_i)$. For $0 \le p \le q \le \tau_i$, the number of i-cells whose age is in the interval $[p,q]$ at time t is $\int_{w=p}^{q} n_i(w,t)dw$. In particular, the total number of i-cells at t is $x_i(t) = \int_{w=0}^{\tau_i} n_i(w,t)dw$. The units by which cells are cunted are normalized so that the initial quantity is $x_i(0) = 1$.

Initially, before treatments begins, it is assumed that the cell ages distribute uniformly along the life cycle, that is, $n_i(w,0) = \frac{1}{\tau_i}$, $w \in [0,\tau_i]$. When chemotherapy is applied, the cell age distribution obtains some non-uniform shape, depending on the treatment schedule.

With no treatment the number of a-cells is assumed to double during each cell cycle, that is, $r_a = 2$. In reality we may find that the actual growth rate is lower. However, a growth rate of 2 defines the worst case scenario, and the solutions found for this case still hold when the rate is lower. The host cells' growth rate depends on their number. The growth rate at time t is $r(x_h(t))$, where $r(x)$ is a (non-linear) decreasing function that tends to 1 as x goes to 1. Therefore, the growth of the host cells slows as they multiply. Note that our model assumes that although influenced by the total number of host cells, their growth rate is independent of the age distribution.

We denote by α_i the proportion of all i-cells that that are destroyed during one time unit of treatment (host or malignant). Note that different rates for h- and m-cells may be eliminated by newly developed drugs that are more aggressive to m-cells than to h-

cells. A treatment policy (schedule) consists of the times at which specific doses are applied.

Any policy that cures the patient without damaging more h-cells than is linically affordable is a good policy, and can be accepted as a solution of high quality to our problem. However, defining a most desirable policy is not an easy task, since both the time of cure, and the number of h-cells at time T determine the quality of a treatment: The relative importance of each one of these factors has to be defined in order to refine the performance of the algorithm. The fitness function constructed to meet these criteria is

$$\begin{aligned} &fitness(s) = (x_h(T) - \beta_h)(2 + \beta_h - x_h(T)) - x_a(T) \\ &+ c_1 I_{alive} + c_2 I_{cured} + c_3 I_{alive} I_{cured} \\ &+ \frac{time\_of\_death}{K}(1 - I_{alive}) - \frac{time\_of\_cure}{K} I_{cured}. \end{aligned}$$

where I_{alive} and I_{cured} are indicator functions stating the patients condition at the end of the treatment period. Detailed analysis of this fitness function follows in Section 2.1.2.2.

Our approach is to compute a regimen through numerical computations since theoretical analysis is possible only for very simplified models (8). To make the process computationally tractable, we measure time and age by discrete units of a given length. To make computations reasonably quick, we divide the cells' cycle into discrete time units, and assume that the number of cells is constant over this unit. Thus, treatment policy consists of the times, $t_1, \ldots, t_m \in [0, T]$, at which treatments are given.

The distribution of the cells' age is generated using the following simulation rule: When no treatment is given, all cells mature by one time unit, and the cells that have reached the end of their cell cycle multiply. When chemotherapy is applied, all cells mature by one time unit, cells that are in the critical phase are reduced by a given fraction, and the cells that have reached the end of their cycle multiply.

The growth rates are calculated using the following rules: The m-cells double their number at each cycle, therefore the m-cell growth rate always equals 2. In contrast, the population of h-cells can never exceed its initial level - there is no uncontrolled growth in the h-cells. Their growth rate is assumed to be the highest number not greater than 2 that will keep the total number of host cells at most 1. This growth rate becomes smaller as the host cells replicate.

2.1.2 Optimization

The generality of the above model renders it computationally intractable. Therefore, good, but not necessarily optimal, solutions were computed by different local search heuristics.

2.1.2.1 Search algorithms

Simulated annealing (SA) is one of the three search heuristics used in the study (9). It is a well-known heuristic (for details see (10-11)). Here, we briefly describe the two other heuristics used in the mentioned study.

Threshold acceptance (TA) is a deterministic version of SA. The difference between the two heuristics lies in the criterion for making a downhill descent - accepting a solution s for which $fitness(s) < fitness(s_0)$, s_0 being the current best solution. In SA, downhill descent is made with a certain probability that depends on $fitness(s) - fitness(s_0)$ and on the temperature that is gradually reduced as the simulated annealing process continues. In TA, the temperature is replaced by a series of descending thresholds $t_0,\ldots,t_n$. A solution s such that $fitness(s) < fitness(s_0)$ will replace s_0 as current solution at stage i of the process if $fitness(s) > fitness(s_0) - t_i$. We refer the reader to (12) for further details.

The TA parameters were tested in the mentioned work by running a series of different instances of the problem, and comparing the performances of the algorithm under

different parameter values. The series of thresholds that was taken was geometrically descending, and several values of a descent rate, noted as the reduction factor, were tried. The threshold was reduced after two complete searches of the entire neighborhood, which is similar to the rule used for reducing the temperature in SA. The algorithm terminates when two consecutive thresholds ended with the same fitness value, which is also similar to the SA termination rule.

Old bachelor acceptance (OBA) is a modification of TA, where the threshold doesn't always decrease. In this method, the threshold depends on the acceptance or rejection of the several most recently tried solutions. The heuristic is described in (13), and was slightly changed to suit the specific problem at hand. Thus, the original algorithm used $T_0 = 0$ as the initial threshold, but here $T_0 > 0$ was used. The reason for this modification is that the first solutions tested, always cause an increase in the fitness, and, therefore, lowers the threshold rapidly. When these consecutive improvements stop, many solutions are rejected till the threshold enables another acceptance.

2.1.2.2 Fitness function

In the generic algorithms each treatment schedule is represented by a binary string of length T. Each bit in this string is equivalent to one time unit, say one hour, where a 0 means that no treatment is applied during this hour, and 1 means that treatment is applied. For example, the string 110001 shows that treatment is applied for 2 hours, following which there is no detectable drug in the system during 3 hours, and again treatment is applied over a period of 1 hour. The length of this string can be determined by the user. Such a string is equivalent to a series of treatments, not necessarily of equal length, with drug-free system at variable intervals.

The fitness of a solution includes several factors: $x_h(t)$ and $x_a(t)$ denote the relative numbers of h- and m-cells, respectively, at time t. We measure these numbers as

proportions which are taken with respect to the initial level, so that by definition $x_a(0) = x_h(0) = 1$. When all m-cells are eliminated we assume that the patient is cured. Our discrete representation of the cell age distribution implies that:

$$x_h(t) = \sum_{w=0}^{\tau_h - 1} n_h(w,t)$$

and

$$x_a(t) = \begin{cases} \sum_{w=0}^{\tau_a - 1} n_a(w,t) & \sum_{w=0}^{\tau_a - 1} n_a(w,t) \geq \beta_a \\ 0 & \sum_{w=0}^{\tau_a - 1} n_a(w,t) < \beta_a \end{cases}.$$

In addition, let us define two indicators (using obvious notation): I_{cured} and I_{alive}, that indicate the patient's status during the treatment series. I_{cured} indicates that at some moment during the treatment, the number of m-cells decreased under the required threshold, and from this point on we considered the patient cured. As mentioned earlier, we assume that once a patient is cured the m-cells do not replicate any longer, so that we consider the tumor totally eliminated. The indicator I_{alive} shows that the patient was alive during the entire treatment period, and that at no time did the number of h-cells decrease below the permitted limit. If the patient is cured, $time\_of\_cure$ is the time elapsing until cure happens, and if the patient dies $time\_of\_death$ is the period until the patient's death.

Our aim is to cure the patient as quickly as possible, when a certain level of h-cells must be maintained throughout the entire treatment period in order not to threaten the patient's life. Until the patient is cured, we attempt to preserve as many h-cells as possible. No more treatments need to be given after the patient is cured, and it is assumed that given sufficient time, the h-cells will recover.

As stated, if the patient is cured, we prefer that cure will occur as early as possible. Similarly, in case of the patient's death, we prefer to delay the death as much as we

can. These preferences are made under the assumption that solutions that prolong a patient's life can be more easily modified into solutions that keep the patient alive.

All these considerations taken into account, the following fitness function was constructed:

$$\begin{aligned} fitness(s) &= (x_h(T) - \beta_h)(2 + \beta_h - x_h(T)) - x_a(T) \\ &+ c_1 I_{alive} + c_2 I_{cured} + c_3 I_{alive} I_{cured} \\ &+ \frac{time\_of\_death}{K}(1 - I_{alive}) - \frac{time\_of\_cure}{K} I_{cured}. \end{aligned}$$

Let us now examine how this fitness function depends on each one of the required variables.

The fitness increases as $x_h(T)$ increases. However, this increase is not linear. The quadratic argument which includes $x_h(T)$ in the function is equal to 0 when $x_h(T) = \beta_h$, and is maximized when $x_h(T) = 1$. Thus, the function changes more rapidly around the critical value of β_h, where h-cells are very valuable, than around the maximal value of 1, where h-cells can easily be spared. Its derivative changes from 2 when $x_h(T) = \beta_h$ to $2\beta_h$ when $x_h(T) =$ 1. Comparing this to the derivative of the argument representing $x_a(T)$ in the fitness function, which always equals 1, we see that many h-cells can be sacrificed in order to eliminate one m-cell when $x_h(T)$ is around 1. When $x_h(T)$ is close to β_h, we will sacrifice an h-cell only if many target cells will be eliminated at the same time. This way, h-cells affect the fitness more when they are most needed.

A ``bonus" of c_1 is given if the patient survives the treatment, and c_2 if the patient is cured. In addition, if both goals are achieved, an additional bonus of c_3 is given. Note that *cured* doesn't necessarily mean *alive*. Two thresholds exist, one for the h-cells and one for m-cells, that determine the patient's status: if the h-cells are reduced below their threshold then the patient is considered dead. If the m-cells are reduced below their threshold, the patient is cured.

Since the effect of the $time\_of\_death$ variable should never exceeds the effect of any of the indicators that were mentioned earlier, its contribution to the fitness is normalized such that it will never be greater than 1. This is done by dividing the $time\_of\_death$ by a constant $K > T$.

Following the same logic, if a patient is cured we would like the cure to occur as early as possible. In this case this demand is not just a means of comparing ``good'' solutions in order to modify them, but an actual benefit to the patient. The contribution of the $time\_of\_cure$ variable is also normalized as mentioned before, for the same reasons.

Possible solutions to the above defined optimization problem are scheduling plans represented by strings of "0"'s (no treatment) and "1"'s (treatment). The possible schedules have been tested by three local search-based heuristics, to find a solution that will locally optimize the fitness function. The comparison between the three approximation methods mentioned above shows that they are competitive, but the computational effort is much higher in SA than in the other two methods. All three methods produced solutions of similar quality and therefore the choice among them should be done according to their computational efficiency.

2.2 Discussion

The general approach for selecting desired chemotherapy schedules, described in the above section, can satisfy a realistically complex medical optimization problem. In order to enable its implementation in the clinic, elaborate mathematical models of pathology and physiology have been developed, yielding precise quantitative predictions of cancer progression and the drug-susceptible physiological processes, notably, hematopoiesis. One of these models describing vascular tumor growth will be briefly described below.

3. Use of Virtual Patient concept to predict improved drug schedules

3.1 Modeling Vascular Tumor Growth

The progress in understanding the biology of tumor neovascularization (angiogenesis) enables formalization of the known properties of this process. A detailed model is required to reflect the role of growth factors (cytokines) in the signaling cascade of tumor vascularization, so as to depict the non-monotonic and unstable angiogenic behavior, observed even under no anti-cancer treatment (14-16).

The first simple model that incorporates the mediating role of angiogenic signaling by tumor cells is explored in Agur et al., (17-18). It consists of three ordinary differential equations (ODEs) describing the dynamics of three variables: the tumor size, N, the concentration of the protein involved in angiogenic signaling, P, and the volume of blood vessels, V.

The tumor growth rate is assumed to depend on nutrient supply, which is proportional to vessel density, defined by $E = V/N$, as follows.

$$\dot{N} = f_1(E)N. \qquad (1)$$

Here, the function f_1 is increasing, $f_1(0) < 0$, $\lim_{E\to\infty} f_1(E) > 0$, i.e., the tumor will regress for zero vessel density and will grow with bounded rate for high vessel density.

The signaling protein is assumed to be secreted by the tumor as a result of nutrient deficiency:

$$\dot{P} = f_2(E)N - \delta P. \qquad (2)$$

Here, the function f_2 is decreasing, $f_2(0) > 0$, $\lim_{E\to\infty} f_2(E) = 0$, i.e., when vessel density is large, the secretion of the pro-angiogenic protein drops, while at small vessel density each tumor cell secretes more protein. The second term accounts for first-order decay of the protein.

The size of the vessels is determined by the protein, as follows:

$$\dot{V} = f_3(P)V. \qquad (3)$$

Here, the function f_3 is increasing, $f_3(0) < 0$, $\lim_{E\to\infty} f_3(E) > 0$, i.e., small amount of protein causes vessel regression, while high amounts induce growth of vasculature.

The model given by equations (1–3) is studied in (17-18) in numerical computations using sigmoid-like functions. It turns out that in contrast to previously published models, here no positive stable biologically relevant steady state exists. Note that the steady state $N = P = E = 0$ is of no interest, since the model describes the dynamics of existing vascular tumors. It was analytically proven in this model that both the tumor and the vessel volume always grow monotonically showing no oscillations. The vessel density can either increase unlimitedly or stabilize at some level, so that the tumor and the vessels grow proportionally. Since these modeled tumor and vascular dynamics fail to capture the full range of the observed real life cancer growth behavior, such as oscillations, one has to consider the introduction of additional assumptions that may enrich the model behavior.

In (17-18) the above model is extended by introducing time delays into the equations. Specifically, it is assumed that the current tumor growth rate and vessel formation rate depend on the prior vessel density and protein concentration some time before. Mathematically, this leads to the following system of delayed differential equations (DDE).

$$\dot{N} = f_1(E(t-\tau_1))N$$

$$\dot{P} = f_2(E)N - \delta P \tag{5}$$

$$\dot{V} = f_3(P(t-\tau_2))V. \tag{6}$$

Here all the functions are the same as in the system of equations (1–3), τ_1 and τ_2 are time delays, so, for example, tumor growth rate depends on vessel density some τ_1 time units ago, rather than depending on the current vessel density. In Agur et al. (17) it is shown that this model exhibits a specific behavior, termed Hopf bifurcation, namely periodic oscillations of tumor size and vessel volume under some specific conditions. Since such behavior is observed in laboratory experiments in untreated animals (19), it can thus be concluded that the system of equations (4–6) is a minimal model able to reproduce the experimentally observed non-monotonic behavior of the angiogenic tumor.

In Bodnar and Forys (20) the models expressed in equations (1–3) and (4–6) are modified by introducing the logistic term into the equation for tumor growth. The addition of this term is justified by the observed deceleration in tumor growth and the existence of natural limit for the tumor size, even if no limitations are imposed by the vascular system. Thus, for the system of equations (1–3) the first equation now becomes

$$\dot{N} = \alpha N\left(1 - \frac{N}{1 + f_1(E)}\right), \tag{7}$$

and for the system of equations with delay (4–6) the first equation becomes

$$\dot{N} = \alpha N\left(1 - \frac{N}{1 + f_1(E(t-\tau_1))}\right). \tag{8}$$

where f_1 is the same as in equation (1) and α is the maximal tumor growth rate. The analysis in (20) shows that these two models always exhibit at least one stable steady state with $N > 0$, thus representing a realistic saturation in tumor growth. The model

with delays also exhibits oscillatory behavior, similar to the model given by equations (4–6).

It should be noted that the simple concept of carrying capacity as used in (21) was replaced in the models presented above by the more elaborated notion of vessel density, reflecting the relationship between the vessel volume and tumor size. In fact, the crucial factor governing tumor growth is the efficiency of the vascular support. To account for this, in (22-23) the notion of effective vessel density (EVD) is introduced. It differs from the previously used vessel density in that it takes into consideration that different types of vasculature can contribute differently to nutrient supply. Following this notion, the blood vessels involved in tumor angiogenesis are divided into two groups – the immature vessels and the mature vessels. The more detailed description of the angiogenic process takes this distinction into account. The new vessels are formed by endothelial cells, which proliferate and migrate upon angiogenic signals. These newly formed vessels are unstable and inefficient in nutrient supply. They are termed immature vessels. However, these vessels can stabilize by undergoing a maturation process, essentially coating the endothelial cells by smooth muscle cells, named pericytes. This process is governed by a different type of molecular signal - the maturation signal. Mature vessels can also destabilize, as a result of decaying maturation signals or the appearance of anti-maturation signals. Experimental observations (14-16) suggest that the dynamics of maturation and destabilization may be responsible for the non-monotonicity in tumor and vasculature growth. Following this suggestion an additional model of five DDEs was proposed in Agur et al. (17). This model describes the growth of immature and mature vessels, V_1 and V_2, respectively, as two inter-related processes. Two types of signaling proteins are considered. The first, P_1 is secreted by tumor cells and assumed to stimulate immature vessels growth. Its role is equivalent to that of P in the previous models. The second protein, P_2 stimulates maturation. It is also assumed to be secreted by tumor cells. This model takes the following form:

$$\begin{aligned} \dot{N} &= f_1\left(E\left(t-\tau_1\right)\right)N \\ \dot{P}_1 &= f_2\left(E\right)N - \delta_1 P_1 \end{aligned} \qquad (9)$$

(10)

$$\dot{P}_2 = aN - \delta_2 P_2 \quad (11)$$

$$\dot{V}_1 = f_3(P_1(t-\tau_2))V_1 - f_4(P_2)V_1 + f_5(P_2(t-\tau_3))V_2. \quad (12)$$

$$\dot{V}_2 = f_4(P_2)V_1 + f_5(P_2(t-\tau_3))V_2. \quad (13)$$

Here equations (9, 10, 12) are similar to equations (4–6), except for the indices of P_1 and V_1 added here. The function f_4, accounting for the maturation rate, is positive and increasing. The function f_5 computes mature vessels destabilization; it is positive and decreases to zero. In addition, the computation of E is changed. Now it depends on both types of vessels, $E = (\alpha_1 V_1 + \alpha_2 V_2)/N$, α_1 and α_2 being the relative contribution of immature and mature vessels to the EVD. In this work, both were taken to be 1. This model also exhibits oscillatory behavior, suggesting the possible role of blood vessels maturation and destabilization in tumor growth.

Finally, a more comprehensive model of the processes discussed above has been developed in order to better represent experiments where human ovary carcinoma spheroid were implanted in mice and tumor growth as well as immature and mature vascular dynamics were monitored in vivo (22-23). This model is formulated in terms of difference equations discrete in time and also, by ODE formalism. The model captures the dynamics of the angiogenic tumor, calculating the following variables over time: tumor size, immature vessels density, mature vessels density, number of endothelial cells, number of pericytes, concentration of Vascular Endothelial Growth Factor (VEGF), concentration of Platelet-Derived Growth Factor (PDGF), concentration of pro-maturation factor Angiopoietin1 (Ang1), and concentration of its competitor, anti-maturation factor Angiopoietin 2 (Ang2). The equations for these variables reflect the biological understanding of the role of the system components, similar to the models described above. We refer the reader to Arakelyan et al., (23) for more detailed description.

In Arakelyan et al. (23) it is shown that, consistent with the simpler models: if the maturation process is neglected, tumor and vasculature growth become monotonic. In

contrast, the introduction of vessel maturation and their destabilization dynamics into the model reduces tumor growth and leads to highly non-monotonic behavior, including irregular oscillations of tumor and vasculature size. Further, by simulating anti-VEGF and anti-PDGF treatments, it was demonstrated that anti-angiogenic treatment alone will not suffice to eliminate the tumor and has to be combined with anti-maturation treatment. As will be described below, this prediction has been corroborated in the pre-clinical setting by showing in pancreatic cancer mouse models that the combination of a VEGFR inhibitor with another distinctive kinase inhibitor targeting PDGFR activity (Gleevec) was able to regress late-stage tumors (24).

In summary, an accurate and detailed description of system dynamics can be obtained using complex models, which account for known relevant components and processes. Even more importantly, mathematical modeling allows one to determine the minimal necessary components required to produce the observed phenomena and to understand how the complex behavior emerges from basic system properties. Once experimentally validated, the model can be used to assist researchers to improve and accelerate drug development and help identify the most promising treatment regimens for different drugs that may subtly vary in drug action mechanism. See **(25)** for a more comprehensive review of the development of angiogenesis models.

3.1.1 A multiscale vascular tumor growth model retrieves the clinical scenario and suggests efficacious regimens

Mathematical analysis and numerical simulations of the Arakelyan et al's 2002 model shed important light on vascular tumor dynamics. Thus, it was suggested that there are circumstances in which small tumors oscillate in size instead of growing steadily. If such circumstances can be medically replicated then this may be a powerful way of controlling cancer growth (23, 26). Notably, it was suggested that monotherapy by anti-angiogenic drugs alone can slow tumor growth, but cannot altogether eliminating it, and that anti-angiogenesis drugs combined with drugs that target mature vessels

may be superior to anti-angiogenic monotherapy (19, 27-28). As was mentioned above, these conclusions were later corroborated experimentally (24).

In order to check whether or not the model is a high-fidelity portrayal of vascular tumor growth, its predictions are to be experimentally validated. This is essential if one is to use the model in the context of the Virtual Patient, where new drugs are examined for their efficacy. In (28), the vascular tumor model was verified in xenograft experiments. Thus. tumor growth, vascular maturation and functionality were studied noninvasively by magnetic resonance imaging (MRI) in human epithelial ovarian carcinoma spheroids, xenografted in mice. Individual tumor growth curves were input into the model for evaluating the tumor-specific parameters, and predictions of vascular dynamics were compared with the MRI readings. The revealed accuracy and critical importance of model predictions is demonstrated by the following example. The model predicts complete maturation of all neovasculatures in a tumor, within about one month. Indeed, the experimental results support model predictions quite remarkably and further explain the model-predicted and clinically-observed short-term effects of the anti-VEGF drug Bevacizumab (29-30)

The accuracy of the mathematical model of vascular tumor dynamics was further validated clinically, by comparing its predictions to the clinical response of metastatic breast cancer (MBC) patients to Docetaxel; this drug is among the few monotherapy options available for patients that are resistant to other alkylating agents. Predicting individual response to Docetaxel may improve the efficacy of treating MBC patients. The mathematical model of solid tumor dynamics, previously validated in preclinical studies, was employed in a retrospective study of MBC patients.

Clinical and histopathological data were collected from 25 MBC patients treated with tri-weekly Docetaxel. The patients were randomly divided into a training set (18 patients), for adjusting population-specific PD, and a validation set (7 patients), for predicting disease progression under individually assigned Docetaxel regimens. Once-weekly Docetaxel regimens were also simulated for the patients and compared with their actual clinical performance.

The model accurately predicted the observed tumor sizes over the entire observation period (R2=0.7; p<0.001) and the objective tumor response assessed according to RECIST (85.7% of match between the observed and predicted, Kappa=0.72, p<0.05; Figure 2). Significantly improved efficacy was predicted for the once-weekly schedule in 48% of the patients. Model analysis revealed that angiogenesis-intensive tumors can be controlled by more frequent Docetaxel dosing, whereas angiogenesis-poor tumors may be treated by less dense regimens (29).

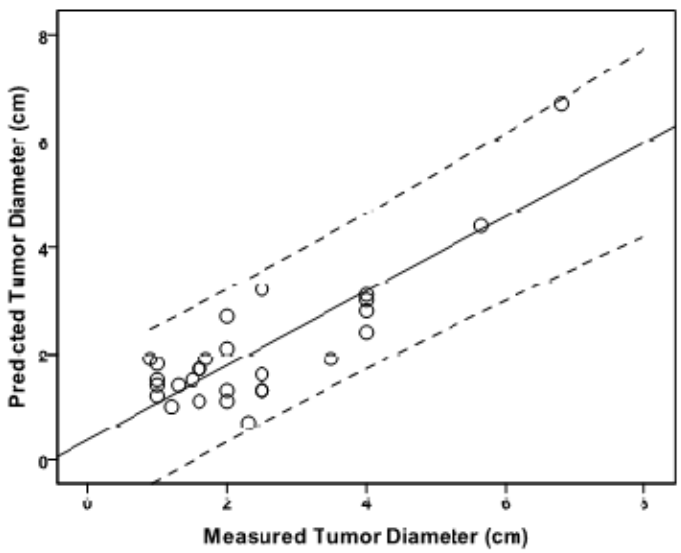

Figure 2. Predicted vs. measured tumor diameter. Prediction accuracy of the vascular tumor model. *Tumor size at the end of treatment, R2=0.7 (p<0.001); objective tumor response assessed according to RECIST; 85.7% (Kappa=0.72, p<0.05). Regression model line (solid line); 95% confidence interval (dashed line).*

3.2 Synthetic Human Population (SHP)

In the preceding sections, we described the concept of the Virtual Patient model using simple models of tumor growth and patient toxicity, as well as optimization problem formalism in order to identify treatment regimens which will maximize drug efficacy while minimizing its toxicity. We were noting that the Virtual Patient can admit more complex biological progression models, and went on to describe the methodology underlying the development of a multi-scale mathematical model for vascular tumor growth. We then pointed out that the use of the Virtual Patient model in drug development requires preclinical and clinical validation, and showed examples of such validation experiments. In the same way as described for the

efficacy model, namely for drug effects on tumor progression, one embeds toxicity models in the Virtual Patient "platform." That is to say that, models describing physiological processes that are known to be target to the drug under study are simulated in parallel to the pathology models and specific optimization problems are then solved, as described above.

To use the Virtual Patient platform in order to predict the effect of a drug treatment on the entire patient population (or sub-population), a Virtual Patient *population* needs to be generated. To this end one must replace the parameters evaluated for a single patient model, by a distribution representing the population distribution of each of the parameter. In practice, the individuals belonging to the "virtual population" share most of the model parameters. However, several parameters are individually selected from a predefined distribution. These parameters and their actual values are selected based on studies indicating that they may have a prognostic value, and given that most of them are readily measured in the laboratory (31-33).

The SHP method is to be employed whenever we wish to generate a larger sample of patients that probes different areas in the parameter space and may also provide higher accuracy in prediction the real population response.

The general definition of the problem to be solved is the following. Given a set of p parameters that is assigned to N individual patients – how to generate a larger set, M >N, of the p parameters such that the statistical properties of the initial set are preserved. Three restrictions should be made. The first determines that the average value of each parameter is the same in the real set and in the SHP set. Secondly, the standard deviation of each parameter in the SHP should reflect that in the real world. Lastly, the covariance matrix in the SHP set should reflect that in the real world.

Three methods for obtaining Virtual Patient populations will be described below. These are Parameter Inflation, Convex Biased Interpolation and Statistical Sampling.

3.2.1 Parameter Inflation ("cherries and flies").

Initially, we define each input "individual" as a point, $\vec{P} \equiv |p_1, p_2, ..., p_n|$, in the parameter hyperspace, according to the parameter values (pi) obtained in the parameter evaluation process. Subsequently, multiple, normally distributed, random points $\vec{R}$, are generated around each of the input "individuals", such that $r_i \sim N(p_i, \sigma_i^2)$, where p_i and r_i, are the values of the i-th input and output parameters, respectively, and σ_i, the standard deviation, determines the degree of variability. Empirically, we have selected σ_i to be between 1% and 5% of the estimated value p_i. This parameter inflation approach is relatively fast and little error-prone.

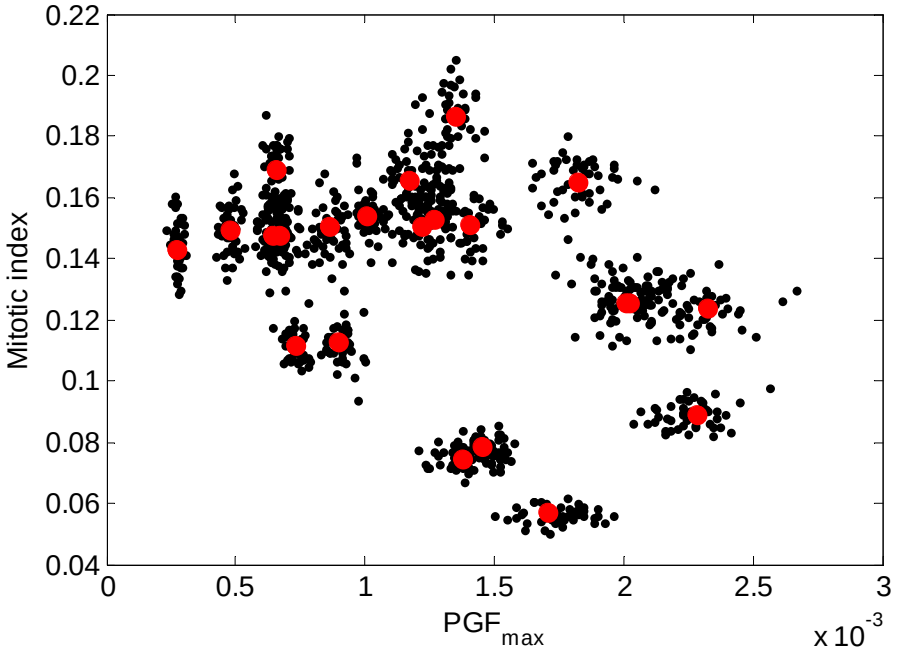

Figure 3. Demonstration of parameter inflation in two dimensions (two parameters). *Thick red points represent values obtained during the parameter evaluation process. Thin black dots represent the generated values. The term "cherries and flies" method was inspired by the shape of this plot.*

3.2.2 Convex Biased interpolation

In this method we generate additional experiments by taking a linear combination of the initial set of χ experiments, as follows

$$E_i = \{P^i_{\{j\}} = \sum_{k=1}^{\chi} r_{i,k} P^k_{\{j\}} : 1 \le j \le N\} : i > \chi$$

.

The requirement that the coefficients, $r_{i,k}: \ 1 \le k \le \chi$, sum up to 1, provides new experiments which fall inside the convex hull, defined by the χ points in the N dimensional space that represents the initial experiments. In other words the parameter range restriction is met.

When the values of $r_{i,k}$ are randomly chosen within the range [0, 1], the parameter values of the resulting new experiments would not meet the standard deviation restriction mentioned above. The standard deviation of the new experiments would be smaller than the one of the original experiments.

To handle the σ restriction, as well as the correlation restriction, the linear combination coefficients $r_{i,k}$, has to be taken from the "tails" of the range [0,1]. This is done by raising $r_{i,k}$ to the power of q_0, $R_{i,k} = (r_{i,k})^{q_0}$, for some constant q_0, where $R_{i,k}$ are normalized

The generated additional experiments are points in the N-dimensional space, located 'close' to the χ points (which stand for the initial "real" experiments) inside their convex hull.

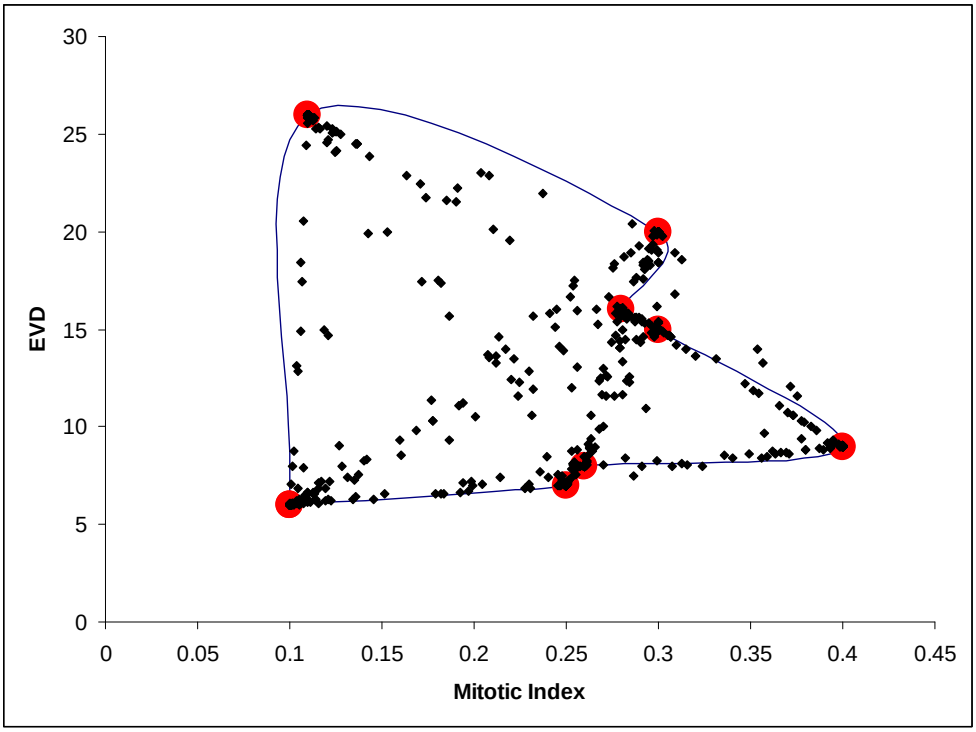

Figure 4. Demonstration of the convex biased interpolation method in two dimensions (two parameters). *Thick red points represent values obtained in parameter evaluation process. Thin black dots represent the generated values.*

3.2.3 Statistical sampling

This method generates a multivariate normal random series. First, we define the distributions of each parameter, p_1.. p_n, by calculating the mean, μ, and variance σ^2 of the estimated values of the observations for each parameter. Then a new set of values for the parameters, p_1.. p_n, can be randomly sampled based on the mean and the covariance matrix of the parameters.

3.2.4 Application considerations

The SHP should not be used when the size of the original real-life population is too small. Specifically, there is no point in trying to generate SHP when the size of the original population is smaller than 10 patients. Moreover, the estimation of the parameter covariance should not be considered reliable when the number of measurements is less than 10 fold the number of independent parameters (e.g. for 3 parameters we have 3 non-diagonal covariance, for 5 we have 10 non diagonal

covariances and for 7 individual parameters we have 21 independent parameters. Thus the non-diagonal covariances should not be considered reliable unless we have at 30 patients for 3 individual variables, 50 patients for 5 individual variables and 210 for 7 individual variables. In the later case, and in general, if the original population is large enough (>100), no SHP is necessary for evaluating the distribution of patients' parameters to be implemented in the virtual patient models which will be simulated.

4. The Interactive Clinical Trial Design (ICTD) algorithm

Above, we have sketched the basic concept of Virtual Patient using very simple model. Subsequently we described the development of more complex and more accurate models for vascular tumor growth, which need to be implemented in the Virtual Patient platform in order to retrieve quantitative predictions of disease progression under drug treatment. We have described methods for enlarging the Virtual Patient to a Virtual Patient population, SHP, in order to represent a specific population of patients, and below we go one step further and briefly describe the Interactive Clinical Trial Design (ICTD) algorithm by which an SHP is used for carrying out virtual clinical trial that predict the response in the various stages of the clinical trials.

4.1 Pre-Clinical Phase: Constructing the PK/PD Module

The pre-clinical phase of drug development concerns the retrieval of the drug's PD and PK in animals and the initialization of human PD research. In this phase a virtual population of the experimental animal, usually that of human cancers xenografted mice, is created, and adjusted to the drug under development, as is detailed below.

Based on the *in vitro* studies, the drug PD module of the virtual animal is constructed. Thus, putative mechanisms of drug action are simulated, retrieving the most appropriate action mechanisms. The mechanism showing best fit to the experimental results is selected as most probable. From the results of the *in vitro* studies, the parameters of the drug's effect on the different target tissues are empirically estimated

and inputted into the module. These include the data of experiments using different tumor types, also in combination with another drug. Inversely, the model here can simulate and comparatively estimate the efficacy of treatment in combination with other known drugs, as well as the effect of the drug on different tumor types. By evaluating parameters to be implemented in the model of the average animal bearing a given cancer disease, and by evaluating the distribution of this parameters in the experimental population, one can create a virtual experimental population, which can direct the pre-clinical research to the most effective avenues. The model is continuously fine-tuned, by "on-line" implementation in the Virtual Animal Population, of the pre-clinical research results. In this way, the model can interactively guide the preclinical research.

Using animal studies, the PK module of the virtual animal is adjusted to describe the PK of the given drug, as evaluated in animal studies. The PD module, which until now was based solely on the *in vitro* data, is adjusted to represent the *in vivo* animal results, and is supplemented by animal parameters for the functions of drug effect time series. This, again, includes data on different tumor types and on the effects of combinations with other drugs. From animals treated by multiple doses, some data on cumulative effect can be obtained and implemented in the model.

The toxicity module is designed on the basis of the qualitative and quantitative data on side effects observed during the animal studies. For example, the Virtual Patient's module describing hematopoietic processes is provided with evaluated values of the parameters of the drug effect on hematopoiesis, if observed in animals. From animals treated by multiple drug doses, some data on cumulative toxicity may be obtained and implemented in the model as well.

At this stage the model already has the capacity to simulate the administration of the drug to humans. Known inter-species differences in the target tissue characteristics are taken into account when simulating the human PK model, in order to consider a reasonable dose range for Phase-I human studies. This procedure is expected to offer

an improvement on the traditional LD10 initial dose for Phase-I trials (the dose lethal for 10% of mice administered drug), which is often too low to show effect on the disease. That is to say that already in this stage, based on *in vitro* and *in vivo* data the model can be used for predicting the minimal dose within therapeutic range, i.e. the lowest dose, which has a rationale to be tested. It is possible at this point to use the model for predicting failure for the drugs with therapeutic doses too toxic to be tolerated.

4.2 Phase-I: Finalizing and Validating the PK/PD Module

During dose escalation testing in the Phase I clinical trials, the PK/PD module in the *Virtual Patient model* is interactively fine-tuned and validated according to the results of the dose escalation experiments. This could, possibly, save steps during dose escalation process, necessary for obtaining the toxicity profile and an initial efficacy profile. During Phase-I trials, while using intra-patient dose escalation method, the model is to be provided with data on cumulative effect and cumulative toxicity, if observed.

In this way, by the end of Phase-I, a fully in vivo verified human model is available, integrating all the existing data on PK and PD of the drug. The general algorithm for conducting interactive clinical trials during Phase I is shown in Figure 5 . In the last stage of the Phase I ICTD work, one uses the SHP formalism to yield a population distribution model for the PK/PD model.

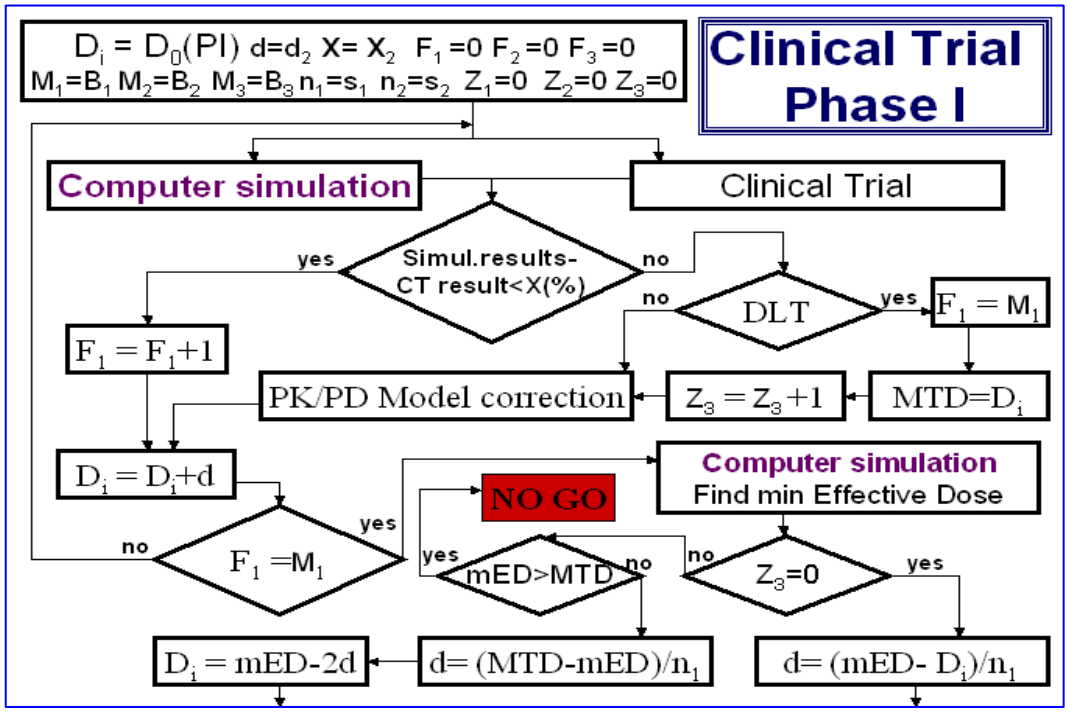

Figure 5. One panel describing the detaled Interactive trial design (out of a total of 12 panels for the whole trial period); *X – a difference between simulated results and clinical trial (CT) results; F1 – a counter;n: D – a "step" for dose elevation; M1 – duration of fit between the simulation to and the clinical observations for model validation; DLT – dose-limiting toxicity; Z3 - a counter; Min Effective Dose (mED) – a dose at which the effect was first observed; MTD – maximal tolerated dose (after which the DLT is observed); n – number of steps to be defined for going from mED* to MTD; NO GO – no rationale to continue *developing the drug.*

4.3 Interim Stage Between Phase-I and Phase-II: Intensive Simulations of Short-Term Treatments

Following Phase-I the model can yield reasonable, short-term predictions for the population effects of specific drug administration schedules on disease progression for specific indications. This allows one to perform an exhaustive search in the regimen space (i.e., within all the treatment schedule possibilities), for those mono- and combination therapy schedules, expected to yield the highest response and lowest toxicity for any potential cancer type to be treated. This may help the drug developer

to predict the most effective treatment schedule and the most promising indication, thus saving patient health, time and cost.

4.4 Phase-II and Phase-III: Focusing the Clinical Trials

At the onset of Phase-II trials and following the interim stage outlined hereabove, a few potential treatment schedules for the selected indication(s) are applied in short pilot trials testing a relatively small number of patients. After the first results are obtained (lasting 6 months, on the average), the SHP model is further adjusted by implementing the new data on the observed effects.

Subsequently, a new set of intensive simulations are carried out, predicting population response to the drug during an extended period of up to two years, and predicting which of the schedules, tested in short-term trials, are expected to yield the best results in the long-run. At this stage the predicted effect for each selected schedule is compared with that of the "Gold Standard" therapy for the same indications.

At this time already, the SHP model can predict failure, that is, recommend a NoGo decision, for the drugs that are incapable of showing benefit over the "Gold Standard" therapy. The schedule(s) predicted to carry the most significant benefit over the "Gold Standard" are selected for further testing in Phase-III. After the efficacy and safety profile of the selected schedule(s) is confirmed in further Phase-II trials (for another 6 months), the selected schedules should be further tested in a larger patient population in Phase-III trials.

The general algorithm of ICTD was compared to a classical clinical trial design of anti-cancer drugs (denoted original). Fig. 6 illustrates the average differences in the number of patients expected to be recruited for the clinical trials designed according to each of the two methods.

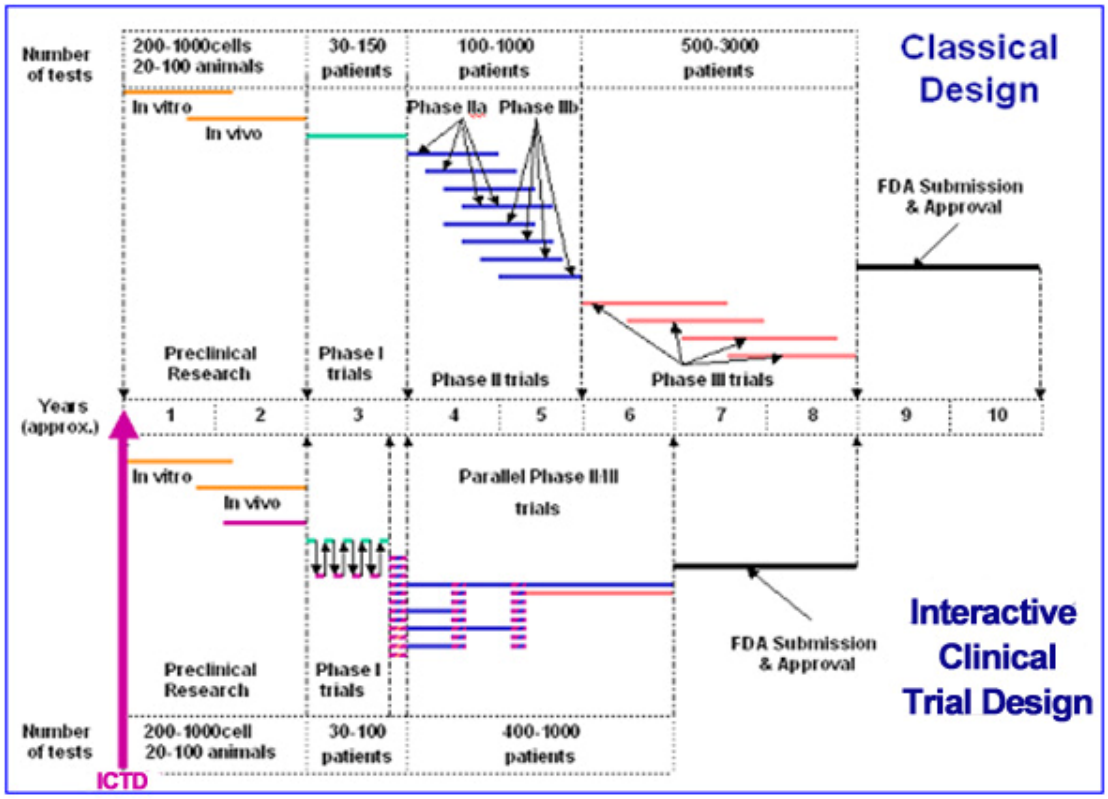

Fig. 6: An illustration of the structure of the Interactive Clinical Trial Design (ICTD) as compared to the classical design for the duration and number of patients *(averages; colors signify different regimens).*

One can notice in figure 6. a significant potential saving in time and in the number of patients, recruited for ICTD. Figure 7A, 7B schematically present the results of our theoretical comparison between the classical design in the development of a, recently approved, drug to be nicknamed "O", which was in development in a big pharmaceutical company and the putative design of the same drug under the ICTD method; the differences (in percentage) in the number of patients and the total duration of drug development are noted at the bottom of each figure.

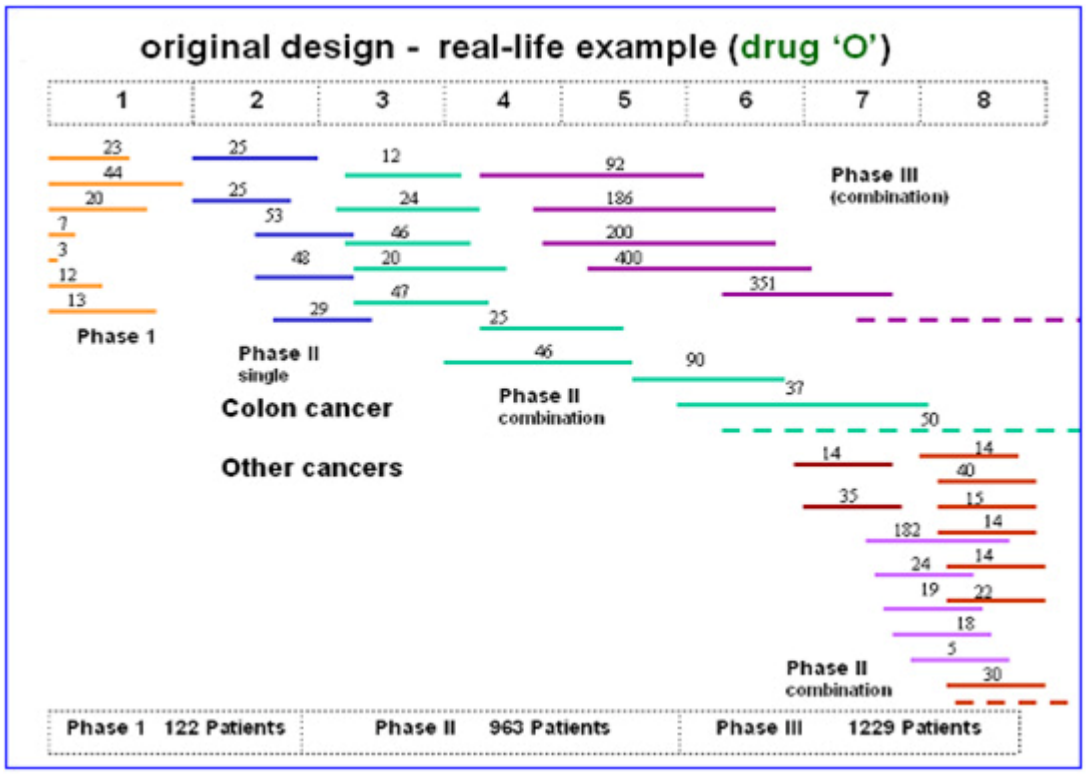

Figure 7A. An illustration of the structure of the classical clinical trial process for drug *"O." Numbers specify number of patients in the specific arm (averages); colors signify different drug regimens.*

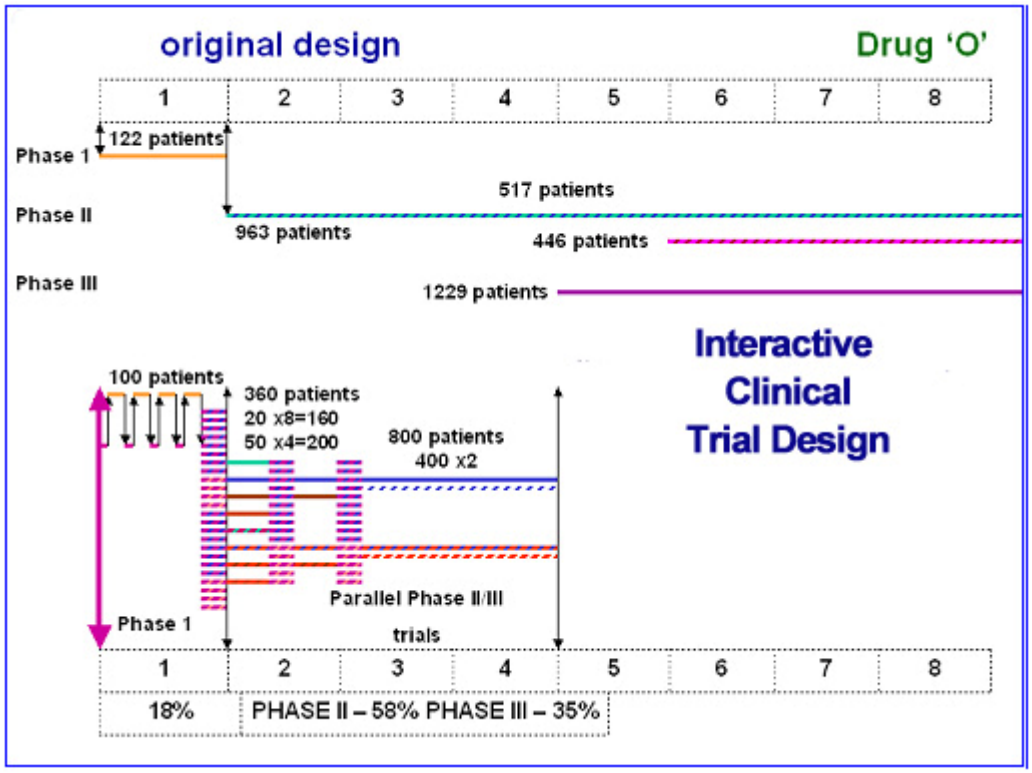

Figure 7B. An illustration of the structure of the classical clinical trial process for drug "O," (summarized; see detail in figure 7A) as compared to the ICTD-proposed trial. *The saving by ICTD depends on the stage when ICTD methodology was implemented; in the current illustration ICTD is implemented in Phase I. Numbers specify number of patients in the specific arm (averages; colors signify different regimens).*

4.5 Interactive Clinical Trial Design (ICTD) method as compared to Adaptive Clinical Trial Design (ACTD) methods

The use of Adaptive Clinical Trial Design (ACTD; Figure 8) methods in clinical research and development has become popular in recent years, due to its flexibility and efficiency. ACTD allows modifications made to trial and/or statistical procedures of ongoing clinical trials. ACTD suggests an improvement to the classical design, as it offers the ability to stop trials relatively early, to drop or add treatment groups, to change group proportions or shift seamlessly into a later phase, etc. These models aid in planning trials by predicting the probability distribution of trial outcomes conditional on current knowledge and assumption, and thus evaluating the ability of

the trial to support a certain decision. These models rely upon prior knowledge on population probability distribution (34-36).

However, since ACTD is based on the assumptions of Bayesian statistics it is a concern that major adaptations of trial and/or statistical procedures of on-going trials may result in a totally different trial that is unable to address the scientific/medical questions the trial intends to answer. We believe that this difficulty is much reduced in the ICTD, which is based on mechanistic models of disease and physiology progression and on the drug mechanism of action and PK/PD, and are therefore significantly less dependent on the trial data than is ACTD.

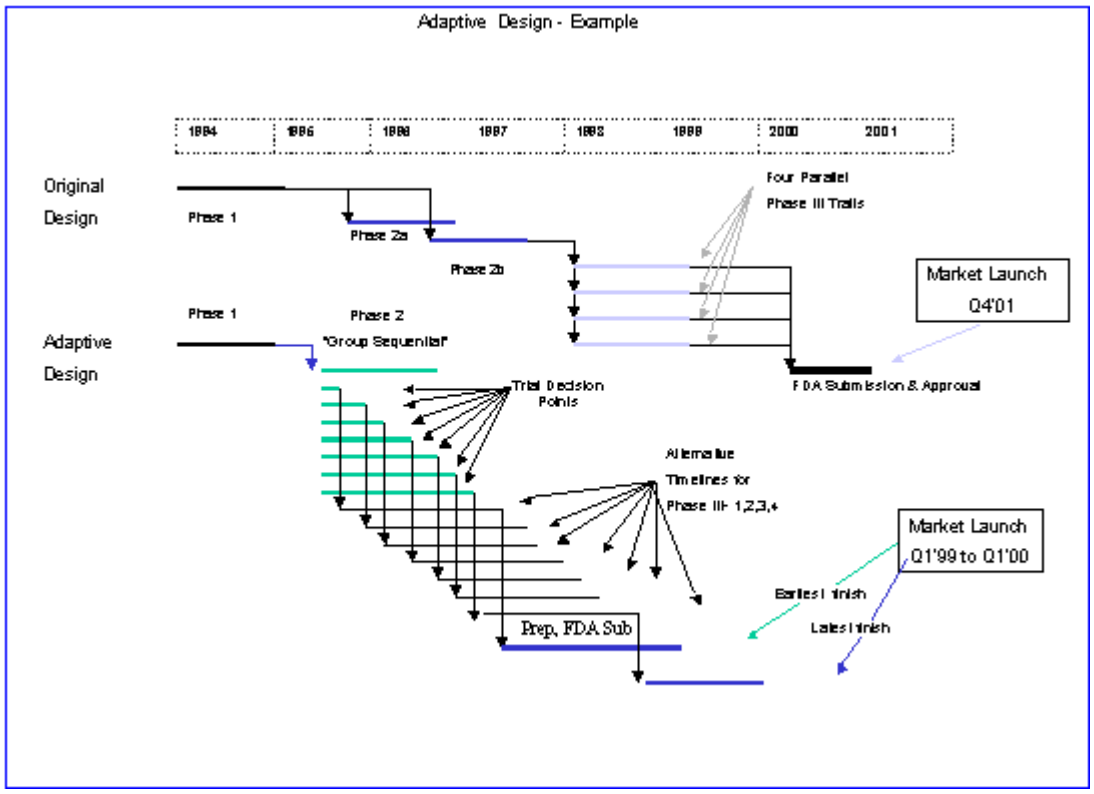

Figure 8. An illustration of the structure of the adaptive Trial Design, as compared to the classical design.

Another significant difference between the ACTD and the ICTD method suggested here lies in the effort in each suggested clinical trial design method. The trials according to ICTD are onset as early as the Pre-clinical stage, or Phase I, whereas those according to the ACTD begin in Phase II. Moreover, while the first and potentially most important decision-making impact of the ICTD takes effect already at the end of Phase-I, the ACTD's impact can be effectuated almost only towards the end of Phase-III. The reason for these differences lies in the significant distinction between the tools employed by each of the designs. The major asset offered by the Virtual Patient technology is the predictive power, rather than the improved data analysis methods, offered by ACTD. In other words, our design is primarily prospective, integrating all the available biological, medical and pharmacological, theoretical and clinical information. In contrast, ACTD is primarily retrospective, integrating statistical methods with the information from the clinical trials.

5. Summary and Conclusions

Drug development is a challenging, costly and time consuming process. Drugs that fail in clinical trials, often due to low efficacy and/or high toxicity levels, are shelved or altogether discontinued. Together with the recent stringency of the regulatory authorities, the high attrition in drug development increasingly exhausts the new product pipelines. Therefore, it becomes mandatory for pharmaceutical companies to revisit their decision-making process at all stages of drug development.

In this chapter we have introduced the concept of the Virtual Patient, and further illustrated its construction by briefly describing mathematical models for tumor progression at different levels of biological detail and at different levels of system complexity. We have described the consideration by which a Synthetic Human Population (SHP) is constructed, that is, a population of Virtual Patients that embodies a specific patient population, and is used to test the potential cost-efficiency of mono- or combination drug therapy. We then described the Interactive Clinical Trial Design (ICTD) method for conducting virtual clinical trials intertwined with and

directing the real-life clinical trials. This method does not replace the Adaptive Clinical Trial Design (ACTD). Rather, we firmly believe that the two methods should be integrated in order to provide drug developers with a comprehensive and powerful tool to navigate drug development towards improved success and improved aid to the well being of our society.

Acknowledgements

I wish to thank L.Arakelyan, R. Ben-Av, R. Hassin, Y. Kogan and S. Levy, for their contribution to the work described in this chapter.

References

1. Agur Z, Arnon R, Schechter B. Effect of the dosing interval on myelotoxicity and survival in mice treated by cytarabine. Eur J Cancer. 1992;28A:1085-90.
2. Cojocaru L, Agur Z. A theoretical analysis of interval drug dosing for cell-cycle-phase-specific drugs. Math Biosci. 1992;109:85-97.
3. Ubezio P, Tagliabue G, Schechter B, Agur Z. Increasing 1-beta-D-arabinofuranosylcytosine efficacy by scheduled dosing intervals based on direct measurements of bone marrow cell kinetics. Cancer Res. 1994;54:6446-51.
4. Agur Z. Resonance and anti-resonance in the design of chemotherapeutic protocols. Journal of Theoretical Medicine. 1998;1:237 - 45.
5. Arakelyan L, Selitser V, Agur Z, inventors; Interactive technique for optimizing drug development from the pre-clinical phases through phase-IV. Pending.
6. Agur Z. The effect of drug schedule on responsiveness to chemotherapy. *Annals NY Acad Sci*. 1986:274-7.
7. Agur Z, Arnon R, Schechter B. Reduction of cytotoxicity to normal tissues by new regimens of cell-cycle phase-specific drugs. Mathematical Biosciences. 1988;92:1-15.

8. Agur Z, Dvir Y. Use of knowledge on {□n} series for predicting optimal chemotherapy treatment. Random & Computational Dynamics 1994;2:279-86.
9. Agur Z, Hassin R, Levy S. Optimizing chemotherapy scheduling using local search heuristics. Operations Research. 2006 54:829-46.
10. Aarts EHL, Lenstra JK. Local search in combinatorial optimization. Chichester England ; New York: Wiley; 1997.
11. Johnson DS, Aragon CR, McGeoch LA, Schevon C. Optimization by Simulated Annealing: An Experimental Evaluation; Part I, Graph Partitioning. Operations Research. 1989;37:865-92.
12. Dueck G, Scheuer T. Threshold accepting: A general purpose optimization algorithm appearing superior to simulated annealing. Journal of Computational Physics. 1990;90:161-75.
13. Hu TC, Kahng AB, Tsao C-WA. Old Bachelor Acceptance: A New Class of Non-Monotone Threshold Accepting Methods. INFORMS JOURNAL ON COMPUTING. 1995;7:417-25.
14. Gilead A, Meir G, Neeman M. The role of angiogenesis, vascular maturation, regression and stroma infiltration in dormancy and growth of implanted MLS ovarian carcinoma spheroids. Int J Cancer. 2004;108:524-31.
15. Gilead A, Neeman M. Dynamic remodeling of the vascular bed precedes tumor growth: MLS ovarian carcinoma spheroids implanted in nude mice. Neoplasia. 1999;1:226-30.
16. Holash J, Wiegand SJ, Yancopoulos GD. New model of tumor angiogenesis: dynamic balance between vessel regression and growth mediated by angiopoietins and VEGF. Oncogene. 1999;18:5356-62.
17. Agur Z, Arakelyan L, Daugulis P, Ginosar Y. Hopf point analysis for angiogenesis models. DCDS-B. 2004 4:29-38.
18. Forys U, Kheifetz Y, Kogan Y. Critical-point analysis for three-variable cancer angiogenesis modeling. Math Biosci Eng. 2005;2:511-25.
19. Arakelyan L, Merbl Y, Daugulis P, Ginosar Y, Vainstein V, Selister V, et al. Multi-scale analysis of angiogenic dynamics and therapy: CRC Press; 2003.

20. Bodnar M, Foryś U. Angiogenesis model with carrying capacity depending on vessel density. 2009.
21. Hahnfeldt P, Panigrahy D, Folkman J, Hlatky L. Tumor development under angiogenic signaling: a dynamical theory of tumor growth, treatment response, and postvascular dormancy. Cancer Res. 1999;59:4770-5.
22. Arakelyan L, Merbl Y, Agur Z. Vessel maturation effects on tumour growth: validation of a computer model in implanted human ovarian carcinoma spheroids. Eur J Cancer. 2005;41:159-67.
23. Arakelyan L, Vainstein V, Agur Z. A computer algorithm describing angiogenesis and vessel maturation and its use for studying the effects of anti-angiogenic and anti-maturation therapy on vascular tumor growth. Angiogenesis. 2002;5:203-14.
24. Bergers G, Song S, Meyer-Morse N, Bergsland E, Hanahan D. Benefits of targeting both pericytes and endothelial cells in the tumor vasculature with kinase inhibitors. J Clin Invest. 2003;111:1287-95.
25. Agur Z, Bloch N, gorelik B, Kleiman M, Kogan Y, Sagi Y, et al. Developing Oncology Drugs Using Virtual Patients of Vascular Tumor Diseases. In: Young D, Michelson, S., editor. Systems Biology in Drug Discovery and Development New York: John Wiley & Sons, Inc; 2010.
26. Arakelyan L, Daugulis P, Ginosar Y, Vainstein V, Selister V, Kogan Y, et al. Multi-scale analysis of angiogenic dynamics and therapy. In: Preziosi L, editor. Cancer Modelling and Simulation: CRC Press, LLC, (UK). 2003.
27. Arakelyan L, Vainstain V, Agur Z. Optimizing anti-angiogenic therapy using mathematical tools. ASCO; 2002; 2002. p. 440a.
28. Vainstein V, Ginosar Y, Shoham M, Ranmar DO, Ianovski A, Agur Z. The complex effect of granulocyte colony-stimulating factor on human granulopoiesis analyzed by a new physiologically-based mathematical model. J Theor Biol. 2005;234:311-27.
29. Agur Z. From the evolution of toxin resistance to virtual clinical trials: the role of mathematical models in oncology. Future Oncol. 2010;6:917-27.
30. Walker EP. FDA Panel Nixes Bevacizumab for Breast Cancer. 2010.

31. Assikis VJ, Do KA, Wen S, Wang X, Cho-Vega JH, Brisbay S, et al. Clinical and biomarker correlates of androgen-independent, locally aggressive prostate cancer with limited metastatic potential. Clin Cancer Res. 2004;10:6770-8.
32. Caine GJ, Ryan P, Lip GY, Blann AD. Significant decrease in angiopoietin-1 and angiopoietin-2 after radical prostatectomy in prostate cancer patients. Cancer Lett. 2007;251:296-301.
33. Maruyama Y, Ono M, Kawahara A, Yokoyama T, Basaki Y, Kage M, et al. Tumor growth suppression in pancreatic cancer by a putative metastasis suppressor gene Cap43/NDRG1/Drg-1 through modulation of angiogenesis. Cancer Res. 2006;66:6233-42.
34. Simon R. Some practical aspects of the interim monitoring of clinical trials. Stat Med. 1994;13:1401-9.
35. Simon R. Bayesian design and analysis of active control clinical trials. Biometrics. 1999;55:484-7.
36. Simon R, Norton L. The Norton-Simon hypothesis: designing more effective and less toxic chemotherapeutic regimens. Nat Clin Pract Oncol. 2006;3:406-7.